The Journal of Experimental Biology 209, 3219-3225
Published by The Company of Biologists 2006
doi:10.1242/jeb.02373

Critical role of zinc in hardening of *Nereis* jaws

Chris C. Broomell[1,*], Mike A. Mattoni[2], Frank W. Zok[2] and J. Herbert Waite[1]

[1]*Department of Molecular, Cellular, and Developmental Biology and* [2]*Materials Department, University of California at Santa Barbara, Santa Barbara, CA 93106, USA*

*Author for correspondence (e-mail: Broomell@lifesci.ucsb.edu)

Accepted 7 June 2006

Summary

Hardening of invertebrate jaws and mandibles has been previously correlated to diverse, potentially complex modifications. Here we demonstrate directly, for the first time, that Zn plays a critical role in the mechanical properties of histidine-rich *Nereis* jaws. Using nanoindentation, we show that removal of Zn by chelation decreases both hardness and modulus by over 65%. Moreover, reconstitution of Zn yields a substantial recovery of initial properties. Modulus and hardness of Zn-replete jaws exceed those attainable by current engineering polymers by a factor of >3. Zn-mediated histidine cross-links are proposed to account for this enhancement in mechanical properties.

Supplementary material available online at
http://jeb.biologists.org/cgi/content/full/209/16/3218/DC1

Key words: biological materials, nonoindentation, histidine, zinc.

Introduction

Like their man-made counterparts, hardened biological materials are tailored to perform given functions. Whether used for support (bone and cuticle), armor (shell and cuticle), or as tools (teeth and stingers), the evolution of hardened materials is driven by the need to maximize mechanical properties, including stiffness, wear resistance, hardness and toughness, while allowing for synthesis under physiological conditions and repair or regeneration throughout an animal's lifetime. These materials are almost exclusively composite with respect to the nature and organization of constituents, allowing for the selection, albeit over an evolutionary time-scale, of those components best adapted for a given function. Taken together, these factors underscore the value of biological systems as models for improvement in synthetic material processing and design.

Most stiff animal tissues with a supporting, protective or aggressive function are mineralized. Bone, antler, shell, spicule and tooth are familiar examples (Currey, 1999). This, however, is not the only blueprint in nature for hard and stiff materials. Invertebrate jaws and mandibles often exhibit hardness and stiffness properties that are comparable to mineralized tissues, with little or no mineral content (Lichtenegger et al., 2002; Lichtenegger et al., 2003). Whereas teeth from higher organisms may contain from 75–95% mineral (by mass), their invertebrate counterparts are predominantly organic; total inorganic load is often below 20% (Currey, 1999; Voss-Foucart et al., 1973). Organic components vary according to species and can include protein, chitin and/or cross-linked phenolic compounds (D. N,. Moses, J. H. Harreld, G. D. Stucky and J. H. Waite, manuscript submitted for publication) (Voss-Foucart et al., 1973).

Potential hardening strategies in invertebrate biting structures have been proposed and include oxidative cross-linking (tanning), control of matrix hydration, and fortification by metal incorporation (Andersen et al., 1996; Currey, 1999; Edwards et al., 1993; Hillerton et al., 1984; Hillerton and Vincent, 1982; Lichtenegger et al., 2002; Lichtenegger et al., 2003; Schofield and Lefevre, 1989; Vincent and Wegst, 2004). However, debate remains regarding their relative contributions to overall mechanical properties.

There are significant data suggesting at least an indirect role of metals in the hardening of invertebrate mandibles (Edwards et al., 1993; Hillerton et al., 1984; Hillerton and Vincent, 1982; Lichtenegger et al., 2002; Lichtenegger et al., 2003; Schofield and Lefevre, 1989; Schofield et al., 2002). For instance, cutting edges of insect mandibles exhibit higher levels of transition metals, usually Zn, than bulk material and are typically twice as hard as the rest of the mandible (Schofield et al., 2002). Moreover, in some species, enhanced hardness is observed only late in development following metal incorporation, presumably after major tanning events have taken place (Schofield et al., 2003). Similar connections between metal content and increased hardness have been established in *Nereis virens*, a marine polychaete common to the Atlantic coasts of North America and Europe. This omnivorous worm is equipped with two jaws mounted on an eversible proboscis, which it uses for grasping and tearing

prey. There is no evidence for any mineral content in *Nereis* jaws. Instead, protein coordinated Zn^{2+} cations are concentrated at the tip and serrated edge of the jaw, accounting for roughly 2% of the total dry mass (Bryan and Gibbs, 1979; Lichtenegger et al., 2003). As with insect mandibles, higher values of hardness and modulus correlate with Zn distribution (Lichtenegger et al., 2003). Despite these correlations, however, it remains unclear whether additional modifications occurring concomitantly with metal incorporation contribute significantly to mechanical properties.

In the present report, the contribution of Zn^{2+} cations to the mechanical prowess of *Nereis* jaws is specifically explored by using nanoindentation to measure the hardness and modulus of the jaws before and after metal chelation. The results clearly demonstrate that the removal of Zn causes significant reductions in these properties. Reintroduction of Zn by soaking in a Zn-rich solution yields a substantial recovery of properties, approaching those of the pristine state. To provide perspective on the efficacy of Zn as a hardening and stiffening agent, comparisons are made with the corresponding properties of a wide array of synthetic engineering polymers.

Materials and methods

Collection and preparation of jaws

Live worms (*Nereis virens* Sars) were purchased from Harbor Bait (Newcastle, ME, USA) and frozen at –80°C upon receipt. Jaws were dissected from fresh-thawed worms and soaked in 5% acetic acid/8 mol l^{-1} urea to loosen soft tissue, which was later removed by gentle scraping. Jaws were rinsed, sonicated in Milli-Q water for 30 min, and allowed to air dry overnight before embedding in Epofix resin (Electron Microscopy Sciences, Hatfield, PA, USA).

Samples for secondary ion mass spectroscopy (SIMS) and nanoindentation were cut on a Leica Ultramictrotome with Diatome diamond knives (Electron Microscopy Sciences) as follows. Initial trimming was done with a Diatome Ultratrim diamond knife with a cutting speed of 100 mm s^{-1} and an incremental feed rate of 1 μm $cycle^{-1}$. To prevent potential sample damage, the final 25 μm of sectioning was completed with a Diatome Histo knife at 1 mm s^{-1} cutting speed with a feed rate of 100 nm $cycle^{-1}$. Because inorganic composition varies within a given jaw, care was taken to ensure that surfaces to be used for comparison were generated from the same regions of similar sized jaws. Samples for nanoindentation were prepared as horizontal cross-sections through the distal portion (tip) of the jaw. Longitudinal sections were used for elemental depth profiling by SIMS. All sample surfaces were confirmed to be clean and free of scratches following inspection by optical microscopy and/or scanning electron microscopy in secondary electron mode.

Zn chelation and reconstitution

Embedded jaws were suspended such that only the tip section of the inverted sample was submerged in treatment solution (50 mmol l^{-1} Tris/100 mmol l^{-1} EDTA, pH 8). Samples were incubated in sealed vessels, with stirring, for 96 h at 25°C and rinsed in 50 mmol l^{-1} Tris Cl (pH 8) for 12 h prior to analysis.

Zn reconstitution was achieved by incubation of pre-depleted jaw surfaces in 100 mmol l^{-1} $ZnCl_2$ for 72 h at 25°C. Samples were rinsed in milli-Q water for 12 h prior to analysis.

Scanning electron microscopy (SEM) and energy dispersive X-ray spectroscopy (EDS)

Microtome-surfaced embedded jaws were mounted on conductive carbon tabs (Ted Pella, Redding, CA, USA) on SEM posts and sputter-coated using a Desk II coater equipped with a gold/palladium target (Moorestown, NJ, USA). Images and 2D elemental maps were collected with a Tescan Vega TS 5130MM thermionic emission scanning electron microscope equipped with an IXRF Systems energy dispersive spectrometer (Houston, TX, USA).

Secondary ion mass spectroscopy (SIMS)

SIMS analysis was performed on a Physical Electronics 6650 dynamic quadrupole instrument (Physical Electronics, Chanhassen, MN, USA). An 8 kV, 50 nA primary beam of O_2^+ ions with a beam diameter of approximately 20 μm was rastered to form craters in the samples. Lateral dimensions of the craters were 100×120 μm. Positively charged secondary ions were detected, with the detection area electronically limited to the central 15% of the crater area to avoid edge effects. A 600 eV electron beam was used to achieve charge compensation. Data were normalized to carbon counts to compensate for a small amount of sample charging observed during the course of analysis.

X-ray photoelectron spectroscopy (XPS)

Samples for XPS were prepared as follows. Pooled *Nereis* jaws were ground with mortar and pestle and washed in Milli-Q water. Approximately 100 mg of jaw powder was incubated with stirring in either 50 mmol l^{-1} Tris-Cl (pH 8) or 50 mmol l^{-1} Tris-Cl/100 mmol l^{-1} EDTA (pH 8) at 25°C for 72 h with buffer changes every 24 h. Powders were washed in Milli-Q water and freeze dried, pressed into 2 mm pellets, and mounted on Cu-tape.

Data were collected on a Kratos Axis Ultra Spectrometer (Chestnut Ridge, NY, USA) using 270 W monochromated Al X-rays at 160 eV and a pass energy of 40 eV. A filament was used to provide low-energy electrons for charge neutralization.

Nanoindentation

Nanoindentation experiments were performed on microtomed surfaces of embedded *Nereis* jaws using a fully instrumented Triboindenter (TriboScope, Hysitron, Minneapolis, MN, USA). Following preparation, all samples were allowed to air dry at ambient temperature overnight. For wet testing, mounted samples were submerged in Milli-Q water and allowed to rehydrate for 3 h prior to analysis. Samples were completely submerged for the duration of the experiment. All measurements were taken using a 90° cube-cornered fluid cell

tip (Hysitron, Minneapolis, MN, USA). This tip has a standard cube-cornered geometry but is mounted on a longer shaft to accommodate testing of samples submerged in a fluid cell. Data were collected as horizontal lines with 10 μm spacing between indents. Indentation load profiles were as follows: load to 500 μN at 100 μN s^{-1}, hold for 60 s, unload at 100 μN s^{-1}. Data were collected in open-loop mode with 1026 points collected for each indent. As there is no feedback control in open-loop mode, applied load decreases slightly during the hold period due to viscoelastic relaxation of the sample. This decrease was accounted for in calculations of hardness and modulus from the unloading portion of the load displacement curve. Indentation locations following treatments were offset by about 10 μm from previous indentations to eliminate mechanical interactions between neighboring indents.

Results

Fig. 1A,B shows a scanning electron micrograph of a *Nereis* jaw along with elemental maps obtained by energy dispersive X-ray spectroscopy (EDS) on a pristine cross-section near the jaw tip. The maps show that both Zn and Cl are distributed relatively uniformly throughout the section while Br (and I, not shown) is localized to the peripheral regions of the jaw. Two regions in the jaw periphery exhibit somewhat lower levels of Zn than the bulk material. This elemental distribution is observed in the majority of analyzed jaws. The corresponding elemental maps following 96 h treatment in buffered Tris (Fig. 1C) or Tris with 100 mmol l^{-1} EDTA (Fig. 1D) at 25°C are also shown. Two features of the EDTA treated samples are noteworthy. (i) The treatment removes most of the Zn from the central region of the section (devoid of Br) and from the peripheral regions with lower initial Zn content. (ii) A concomitant loss in Cl is obtained in the Zn-depleted regions, despite the presence of Cl in the treatment solution, but not in the peripheral regions where Zn remains. This suggests that Zn coordination is necessary for Cl retention and is consistent with earlier work that indicates the presence of a $Zn(His)_3Cl$ coordination complex in *Nereis* jaws (Lichtenegger et al., 2003). Control experiments on jaws treated only in buffered Tris showed no appreciable change in jaw composition.

Although the preceding observations are representative of the vast majority of analyzed jaws (*N*=20), there were a few instances in which the Br distribution was uniform over the entire cross-section, whereas I remained localized to the near-surface region (Fig. 2A). In these samples, no significant Zn loss was detected following treatment with EDTA (Fig. 2B), consistent with the behavior of the Br-rich near-surface regions of the other jaws. Two possible explanations for these results are proposed, based on recent isolation of halogenated (histidine and tyrosine) and cross-linked (tyrosine) amino acids from *Nereis* jaw hydrolysates (Birkedal et al., 2006): (i) brominated histidine might exhibit stronger metal binding characteristics, thus preventing chelation (Auffinger et al., 2004; Wang et al., 1994); (ii) protein cross-links arising concomitantly with bromination may render coordination sites physically inaccessible to chemical modification. To partially address this question, X-ray photoelectron spectroscopy (XPS) was performed on pulverized jaws following the aforementioned treatments. Spectra obtained from jaw powders treated with Tris alone were comparable to untreated samples. In contrast, Zn levels were significantly reduced in powders treated with EDTA, whereas other inorganic constituents were largely unchanged (supplementary material, Fig. S1). This indicates

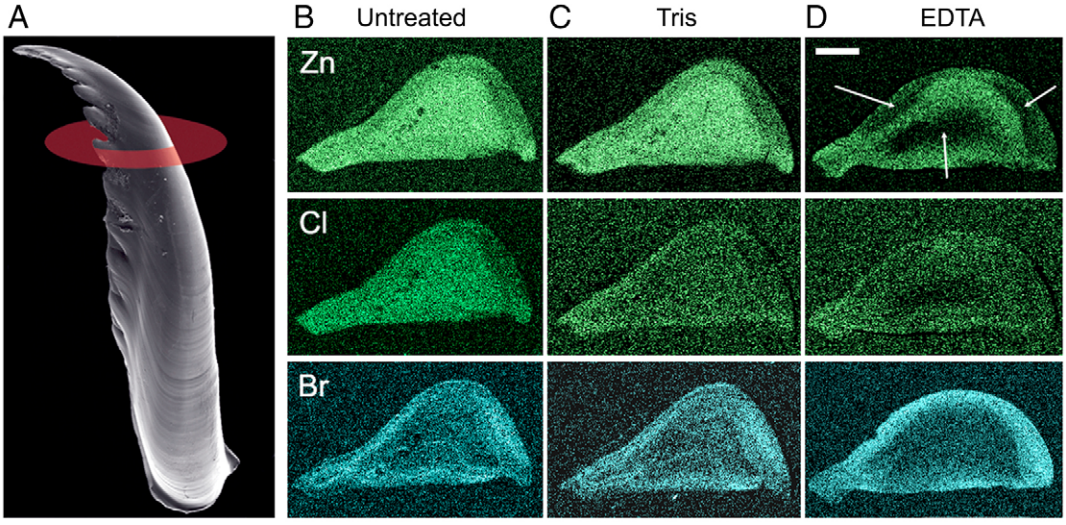

Fig. 1. Distribution of major inorganic components in a *Nereis* jaw cross section. (A) Scanning electron microscopy (SEM) image of a complete *Nereis* jaw. Embedded jaws were prepared by trimming to the plane indicated (red disc) with a diamond knife. Energy dispersive X-ray spectroscopy (EDS) maps of (B) untreated, (C) Tris-treated and (D) EDTA-treated jaw surfaces. Untreated and Tris-treated images are of a single jaw (EDTA treatment was done on a different jaw – distributions of Zn, Cl and Br prior to EDTA treatment were indistinguishable to those in untreated jaws). EDTA treatment, but not incubation in Tris alone, removes Zn and Cl in three distinct regions of the jaw cross section (white arrows). Zn loss is more prevalent in Br-free regions of the sample. Scale bar, 100 μm (cross sections only).

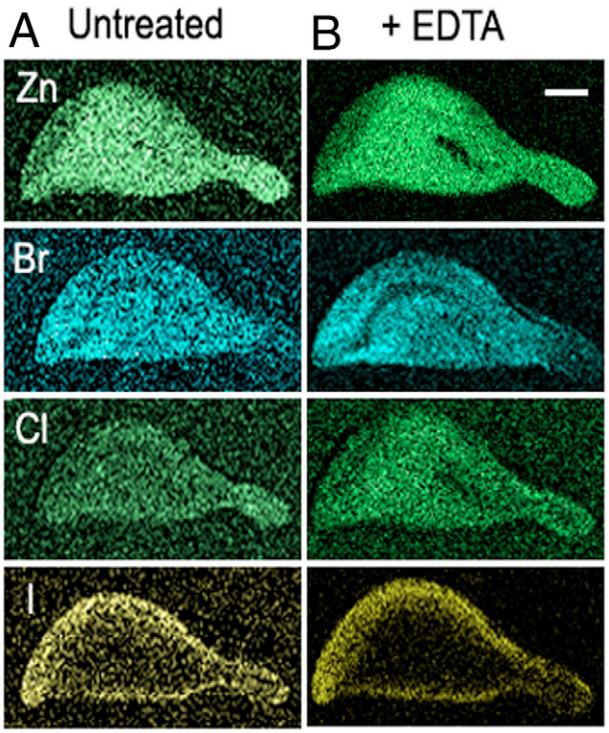

Fig. 2. Effects of EDTA treatment of jaws with uniform Br distribution. (A) Untreated, (B) EDTA-treated jaws. A minority of jaws analyzed exhibited uniform Br levels through the cross section. All other inorganic components exhibit standard distribution profiles (A). Treatment of these samples with EDTA does not lead to Zn or Cl loss. This suggests that bromination (or associated processes) may play a role in stabilizing metal coordination in the jaw matrix. Scale bar, 100 μm.

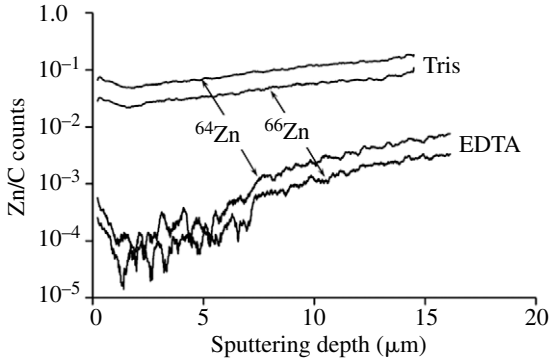

Fig. 3. Secondary ion mass spectroscopy (SIMS) depth profiles of Zn following EDTA treatment. EDTA treatment results in significant decrease of Zn in the top 16 μm of the jaw surface compared with the values observed after Tris treatment. Measurements were taken in regions that were free of Br, and Zn counts were normalized to carbon to compensate for fluctuations in signal intensity throughout the course of analysis. Signal traces for both Zn isotopes are presented.

that mechanical disruption of the jaw matrix is sufficient for near complete Zn removal, thus supporting the model of cross-link mediated metal entrapment in Br-rich regions.

Confirmation of Zn-depletion was obtained by secondary ion mass spectroscopy (SIMS). EDS maps were used to determine appropriate regions for analysis (supplementary material, Fig. S2). Representative results are plotted on Fig. 3. In those regions where Zn depletion had been found, the Zn/C ratio was about two orders of magnitude lower than in similar areas from jaws treated in buffered Tris alone. Br-rich regions near the jaw periphery exhibited some reduction in the Zn/C ratios relative to the pristine jaws, but not nearly as large as those of the central regions (data not shown).

The Young's modulus (E) and hardness (H) of the jaws were obtained by nanoindentation, following the method of Oliver and Pharr (Oliver and Pharr, 1992; Oliver and Pharr, 2004). Briefly, the sample is loaded with a cube-cornered diamond tip to 500 μN and held for 1 min (to allow for visco-elastic relaxation) before unloading. Fig. 4 depicts a standard load displacement curve for a dry *Nereis* specimen. H and E are determined from the unloading portion of the curve; E is related to the slope of initial unloading segment and H is a function of tip displacement at maximum load. Values are calculated based on comparison with an independent multipoint calibration using standards of known H and E. Measurements were made both on dry samples in ambient air and on samples submerged in water. In pristine jaws in the dry state, the properties were uniform across the cross-section, with average values E=12.0(±1.02) GPa and H=0.82(±0.04) GPa (N=174 indents on a single specimen, numbers in parentheses represent s.d.). These values are comparable to (but slightly higher than) those reported previously for *Nereis* jaws, obtained using a slightly different measurement technique: E=9.8 GPa and H=0.54 (Lichtenegger et al., 2003). When submerged in water, the properties were reduced by only about 18%: E=9.9(±1.87) GPa and H=0.68(±0.12) GPa (N=335 total indents on three specimens). Although care was taken to ensure that sample preparation was consistent between jaws, minor variations (i.e.

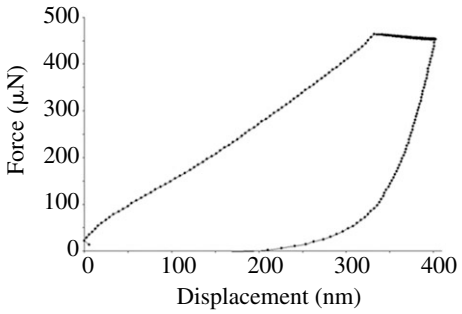

Fig. 4. Nanoindentation of dry *Nereis* jaw surface. Representative load–displacement curve from nanoindentation of a prepared jaw from *Nereis*. Surfaces were indented with a 90° cube-cornered diamond tip at 100 μN s^{-1} to a maximum load of 500 μN and held for 1 min. Decrease in force axis indicates viscoelastic relaxation of the sample prior to unloading. Hardness is determined as a function of the total displacement of the tip into the sample. Modulus is derived from the slope of the unloading curve.

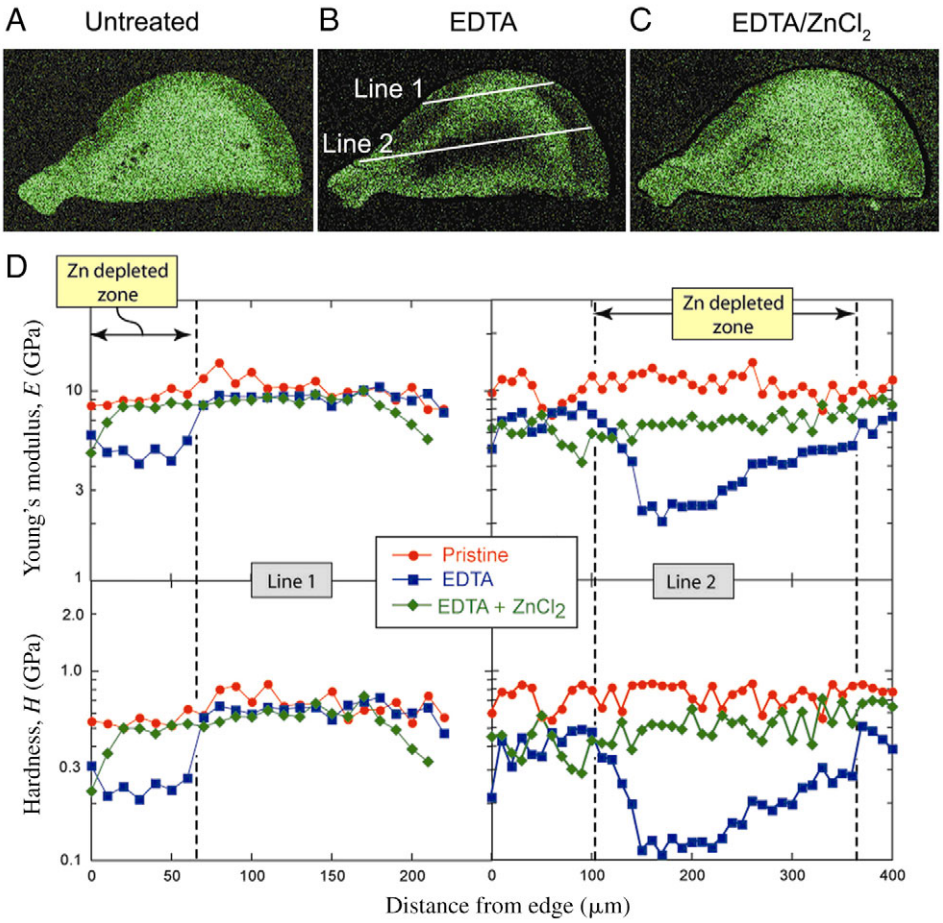

Fig. 5. Chemical and mechanical characterization of *Nereis* jaws following Zn manipulation. EDS Zn maps of jaw cross sections (A) before treatment, (B) after treatment with EDTA and (C) following treatment in $ZnCl_2$. Indents were made following each treatment in regions indicated by the white lines (B). Both lines include indents in Zn-depleted and Zn-rich zones. (D) Hardness, *H*, and Young's modulus, *E*, are presented as a function of lateral position across the sample surface. Comparison of untreated (red line) and EDTA treated (blue line) samples indicates that both *H* and *E* are substantially decreased in regions where Zn has been removed. A significant recovery of initial *H* and *E* is observed following reconstitution of Zn in these regions (green line).

position of the test surface with respect to jaw tip, underlying fiber orientation, etc.) are unavoidable and are reflected in the higher s.d. observed in wet testing.

Effects of Zn depletion on the mechanical properties were ascertained by comparing hardness and modulus profiles across jaw sections before and after metal chelation. Three sets of mechanical measurements (in water) and the corresponding EDS maps are shown in Fig. 5. In the untreated jaws (Fig. 5A,D), the properties are relatively uniform across the section (as noted earlier). In contrast, following metal chelation, both the modulus and hardness are reduced significantly in those regions devoid of Zn (Fig. 5B,D). The average values in the latter regions are E=3.72±1.11 GPa and H=0.18±0.06 GPa: less than 1/3 of the values measured prior to treatment. Paired student *t* tests demonstrate that the differences are statistically significant. Considerably smaller reductions in properties were

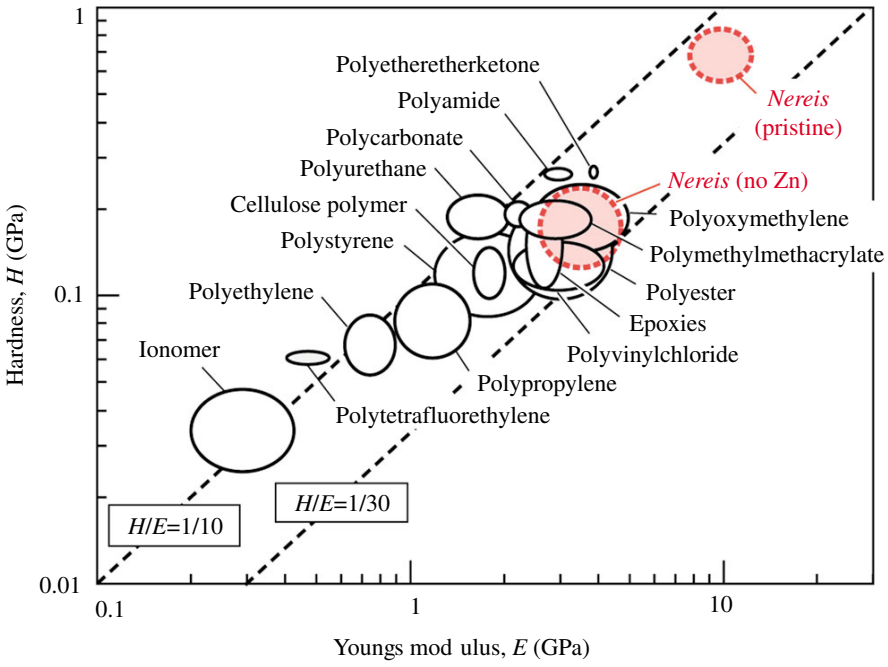

Fig. 6. Comparison of *Nereis* jaws to synthetic engineering polymers. Shown is a materials property chart comparing hardness *H* and Young's modulus *E* of *Nereis* jaws (in water) (pristine and without Zn) with those of synthetic engineering polymers. Theoretical limits for these properties are represented by the broken lines.

obtained in the near-surface regions, consistent with the slight Zn loss evident in the SIMS measurements. Similar measurements on control samples (treated with buffered Tris only) showed no significant change in properties (supplementary material, Table S1).

The potential for reversing the property degradation caused by Zn removal was probed by soaking the chelated samples in 100 mmol l^{-1} $ZnCl_2$ for 72 h and repeating the nanoindentation measurements. Significant (although somewhat incomplete) restorations of both Zn and Cl were evident in the EDS measurements (Fig. 5C). Concomitantly, both the modulus and the hardness were restored to a significant fraction of their initial levels (Fig. 5D). The lack of full recovery may be due to an inability to fully reconstitute available coordination sites over the duration of the soak. Nevertheless, the results clearly demonstrate the reversible nature of the hardening associated with the Zn. These data provide conclusive evidence that Zn binding is critical for the observed measured hardness and stiffness in *Nereis* jaws.

Discussion

Despite several decades of investigation, there is still considerable debate concerning the mechanisms responsible for sclerotization of invertebrate tissues. Three primary mechanisms have been proposed: matrix cross-linking, local dehydration and metal incorporation. Debate persists due to the relative intractability of these systems to direct investigation. In proposing their models, investigators have relied on correlating hardening and stiffening either to secondary evidence of physical modification (e.g. identification of chemical adducts implicated in cross-linking), or to changes in mechanical properties following *in vivo* maturation of the structures (including water loss and/or metal incorporation). Significantly, many tissues bear evidence of multiple strategies, further hindering direct assessment of a given sclerotization model.

We have investigated the role of Zn in hardening and stiffening in *Nereis* jaws. Zinc removal resulted in over 65% reduction of these properties in relevant areas and its reintroduction resulted in their appreciable recovery. To our knowledge these are the first data directly demonstrating that metal incorporation, in the absence of any additional modifications, significantly enhances mechanical properties of invertebrate jaws.

It is possible to suggest that the presence of modified tyrosine and histidine residues from *Nereis* indicates that multiple sclerotization mechanisms might be factoring into jaw mechanics. Prior to treatment, hardness and modulus are relatively uniform throughout the jaw, despite somewhat lower Zn levels near the jaw periphery. We contend, however, that our data and interpretations are valid based on the following factors. (i) All tests were conducted under identical hydration conditions. (ii) EDTA treatment removes only divalent cations from the system; no covalent cross-links are affected (Dawson

Fig. 7. Schematic of proposed cross-linking in *Nereis* jaws. Zn-mediated cross-linking of histidine-rich proteins is proposed to be responsible for enhanced hardness and modulus in *Nereis* jaws. Cross-linking may be intramolecular (black complexes) or intermolecular (grey complexes). Additional cross-linking *via* di-and/or tri-tyrosine formation is not expected to contribute significantly to mechanical properties of the bulk jaw.

et al., 1986). (iii) Although levels are lower than in the bulk jaw, a significant amount of Zn is still present in the jaw periphery prior to EDTA treatment. Both hardness and modulus decrease in these regions following treatment. These data suggest that lower initial Zn levels are sufficient to reinforce the jaw periphery and are consistent with our model for Zn-mediated fortification. (iv) In all tests, decreases in hardness and modulus were only observed in regions exhibiting significant Zn removal. (v) Most importantly, reintroduction of Zn into the jaw significantly restores both hardness and modulus. We propose that the aforementioned amino acid modifications have an alternative function in the jaw. It is possible that cross-linking in the jaw periphery enhances jaw resistance to degradation by enzymes of the worm gut. Similarly, halogenation in these areas may provide protection against bacteria in the gut or seawater.

For a broader perspective, the properties of the *Nereis* jaws before and after metal chelation are compared with those of other macromolecular materials, notably engineering polymers (Fig. 6) (Ashby, 1999). In the latter systems, properties are dictated largely by intermolecular bonds and their associated glass transition temperature, T_g, relative to the measurement temperature. For instance, T_g for linear polymers like polyethylene and polypropylene lies near room temperature and thus both the modulus and the hardness are low. In contrast, for linear polymers with T_g values well above room temperature, such as polymethylmethacrylate and polyamide, the properties are significantly higher. Moreover, hardness and modulus move in tandem, both increasing with T_g. In samples without defects, the theoretical upper limit on their ratio is $H/E \approx 1/10$. Indeed, the data for most polymers fall within the range $1/30 < H/E < 1/10$ (indicated on Fig. 6). The upper limits on these properties, dictated by the strengths of the hydrogen and van der Waals bonds at low temperatures ($\ll T_g$), are $E \approx 4$ GPa and $H \approx 0.25$ GPa. Even network polymers, such as epoxy and polyester, exhibit the same upper limits, also dictated by the strengths of the intermolecular bonds. Interestingly, both the modulus and the hardness of the *Nereis* jaws following metal chelation fall into the upper range accessible by engineering polymers. In contrast, the properties of the pristine jaws are clearly set apart from the others; both the modulus and the hardness are about three times greater than those of even the best engineering polymer. In a similar vein, Schmitt et al. showed that a force of 28 pN was required to repeatedly lift cantilever-tethered Zn^{2+} from a 'lawn' of hexahistidines (Schmitt et al., 2002). These comparisons support the view that Zn in *Nereis* jaws increases the strength of the intermolecular bonds.

Although *Nereis* jaws exhibit hardness and stiffness appropriate for specialized grasping and biting structures, these properties are not dependent on the deposition of mineral, as in the teeth of most other organisms. Instead, based on both the present mechanical measurements and the chemical analyses reported elsewhere (Lichtenegger et al., 2003), hardening and stiffening appear to be mediated by reversible Zn binding of bundles of histidine-rich protein fibers (Fig. 7). The preceding comparisons suggest that substantial increases in hardness and modulus of synthetic polymers might be attained using analogous chemical modification strategies.

The authors would like to thank T. Mates and R. Khan for assistance with XPS data acquisition and interpretation. This work made use of the Materials Research Lab Central Facilities supported by the MRSEC Program of the National Science Foundation under award No. DMR05-20415. This research was funded by NIH BRP DE014672 (overall PI, J.H.W.).

References

Andersen, S. O., Peter, M. G. and Roepstorff, P. (1996). Cuticular sclerotization in insects. *Comp. Biochem. Physiol.* **113B**, 689-705.

Ashby, M. F. (1999). *Materials Selection in Mechanical Design* (2nd edn). Oxford: Butterworth-Heinemann.

Auffinger, P., Hays, F. A., Westhof, E. and Ho, P. S. (2004). Halogen bonds in biological molecules. *Proc. Natl. Acad. Sci. USA* **101**, 16789-16794.

Birkedal, H., Khan, R. K., Slack, N., Broomell, C., Lichtenegger, H. C., Zok, F., Stucky, G. D. and Waite, J. H. (2006). Halogenated veneers: protein crosslinking and halogenation in the jaws of *Nereis*, a marine polychaete worm. *Chembiochem*, in press.

Bryan, G. W. and Gibbs, P. E. (1979). Zinc – a major inorganic component of nereid jaws. *J. Mar. Biol. Assoc. UK* **59**, 969-973.

Currey, J. D. (1999). The design of mineralised hard tissues for their mechanical functions. *J. Exp. Biol.* **202**, 3285-3294.

Dawson, R. M. C., Elliott, D. C., William, H. E. and Jones, K. M. (1986). *Data for Biochemical Research* (3rd edn). Oxford: Oxford University Press.

Edwards, A. J., Fawke, J. D., McClements, J. G., Smith, S. A. and Wyeth, P. (1993). Correlation of zinc distribution and enhanced hardness in the mandibular cuticle of the leaf-cutting ant *Atta sexdens rubropilosa*. *Cell Biol. Int.* **17**, 697-698.

Hillerton, J. E. and Vincent, J. F. (1982). The specific location of zinc in insect mandibles. *J. Exp. Biol.* **101**, 333-336.

Hillerton, J. E., Robertson, B. and Vincent, J. F. V. (1984). The presence of zinc or manganese as the predominant metal in the mandibles of adult, stored-product beetles. *J. Stored Prod. Res.* **20**, 133-137.

Lichtenegger, H. C., Schoberl, T., Bartl, M. H., Waite, J. H. and Stucky, G. D. (2002). High abrasion resistance with sparse mineralization: copper biomineral in worm jaws. *Science* **298**, 389-392.

Lichtenegger, H. C., Schoberl, T., Ruokolainen, J. T., Cross, J. O., Heald, S. M., Birkedal, H., Waite, J. H. and Stucky, G. D. (2003). Zinc and mechanical prowess in the jaws of *Nereis*, a marine worm. *Proc. Natl. Acad. Sci. USA* **100**, 9144-9149.

Oliver, W. C. and Pharr, G. M. (1992). An improved technique for determining hardness and elastic modulus using load and displacement sensing indentation experiments. *J. Mat. Res.* **7**, 1564-1583.

Oliver, W. C. and Pharr, G. M. (2004). Measurement of hardness and elastic modulus by instrumented indentation: advances in understanding and refinements to methodology. *J. Mat. Res.* **19**, 3-20.

Schmitt, L., Ludwig, M., Gaub, H. E. and Tampe, R. (2002). A metal-chelating microscopy tip as a new toolbox for single-molecule experiments by atomic force microscopy. *Biophys. J.* **78**, 3275-3285.

Schofield, R. M. S. and Lefevre, H. (1989). High-concentrations of zinc in the fangs and manganese in the teeth of spiders. *J. Exp. Biol.* **144**, 577-581.

Schofield, R. M. S., Nesson, M. H. and Richardson, K. A. (2002). Tooth hardness increases with zinc-content in mandibles of young adult leaf-cutter ants. *Naturwissenschaften* **89**, 579-583.

Schofield, R. M. S., Nesson, M. H., Richardson, K. A. and Wyeth, P. (2003). Zinc is incorporated into cuticular "tools" after ecdysis: The time course of the zinc distribution in "tools" and whole bodies of an ant and a scorpion. *J. Insect Physiol.* **49**, 31-44.

Vincent, J. F. V. and Wegst, U. G. K. (2004). Design and mechanical properties of insect cuticle. *Arthropod Struct. Dev.* **33**, 187-199.

Voss-Foucart, M., Fonze-Vignaux, M. and Jeuniaux, C. (1973). Systematic characters of some polychaetes (Annelida) at the level of the chemical composition of the jaws. *Biochem. Syst.* **1**, 119-122.

Wang, J. D., Collange, E., Aymes, D. J., Paris, M. R. and Fournaise, R. (1994). Physicochemical properties of iodo-histidines.1. Protometric study of the complexation of metallic cations Cu(Ii), Co(Ii), Ni(Ii), Cd(Ii), Zn(Ii) by monoiodohistidine and diiodohistidine. *Bull. Soc. Chimi. Fr.* **131**, 30-36.